Whitened Merger-Waveform Autocorrelation Functions: Implications for Inspiral Event Localization in Advanced LIGO

LIGO-T080312-00-0

Ashley King, Kipp Cannon
California Institute of Technology

December 28, 2008

Abstract

In this paper, we will discuss the autocorrelation functions of inspiral merger-waveforms to gain insight into the directional localization ability of Advanced LIGO observatories. To do so, we start with the proof that the array of observatories can be approximated as a synthetic aperture imaging system, which creates an "image" of the gravitational wave source. We present these images and discuss the localization that can be inferred from these functions. Finally, we discuss the relationship between this method and the coherent step of IHOPE to model the directional sensitivity for this analysis pipeline.

1 Introduction

As gravitational waves are detected, the position of these sources will lend itself to further analysis of the event. This greater understanding of the event can be deduced by focusing a telescope toward the source in hopes of observing the electromagnetic counterpart. The electromagnetic counterpart will be constrained to a small region, so one must first assess the feasibility of localizing a source to a precise region in which a telescope is sufficient in making an observation. This analysis can be done by using the coherence between the gravitational signals from the various gravitational wave observatories to find its position.

The current coherent step in the Inspiral Hierarchal Online Pipeline Executor (IHOPE) allows for the signals from individual observatories to be combined coherently. This is enabled through maximization over an eight parameter space. These characteristic parameters include the time of arrival, t_a, the phase of the merger, ψ, the inclination of the system, ϵ, the distance to the merger, R, time of final coalescence, t_c, chirp time, ξ, and the position angles $\{\theta, \phi\}$[1]. Of the eight parameters, the position angles are the most pertinent to this study and are found using the time-delay between the incident gravitational wave at a fiducial detector and each subsequent detector. The angle θ is found by,

$$\theta = \sin^{-1}(\frac{c}{d}\Delta t) \tag{1}$$

where c is the speed of light, d is the distance between two detectors, and Δt is the time-delay. However, though θ can be determine, ϕ can not be determined with just one pair of detectors. ϕ thus produces a "great circle" in which the source can lie on the sky for all values of ϕ, and a single value of θ. By using two pairs of detectors, one can limit the source to two sky positions where the two great circles intersect. Furthermore, by using three or more pairs of detectors one can break this degeneracy and determine the location of the inspiral event[1].

In this paper we use the knowledge of the delays between detectors to model the coherence by using the observatories as a synthetic aperture imaging system. This aperture can produce an "image" by correlating the gravitational signals with one another and optimizing the proper time-delay[2]. The "image" allows us to locate the position of the source, and the fringe patterns determine the accuracy of localization. After discussion of the proof behind this approach, we present the "images" as produced by the auto-correlation functions for both neutron star mergers and black hole mergers, whitened by the theorized Advanced LIGO power spectral density (PSD). Furthermore, we present the autocorrelation functions between waveforms as they are produced in the IHOPE coherent step, so as to simulate the most current analysis procedures. The goal of

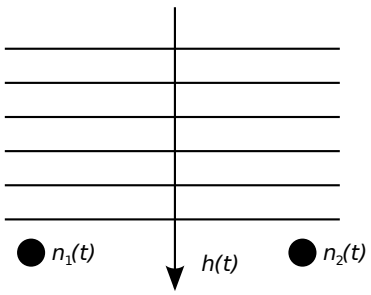

Figure 1: Gravitational wavefronts incident upon two detectors, each of which is a source of noise.

this study serves as a reference for those who seek the direction localization ability for Advanced LIGO detectors.

2 Methods

2.1 Synthesis Imaging of Binary Mergers

One means of assessing the direction-finding capabilities of a network of gravitational wave antennas is to treat the network as a synthetic aperture imaging system, and compute the aperture's beam profile. Imagining the network to form an image of the gravitational wave sky, the width of the central peak of the beam profile sets the spot size in the image resulting from a point source of gravitational waves.

In a synthetic aperture imaging system consisting of point detectors, the image is formed by taking the detector outputs pair-wise and computing the correlation as a function of the relative delay between the signals. The magnitude of the correlation is interpreted as a "brightness", and different delays correspond to different directions for the incident radiation. The images from the different detector pairs are summed linearly. The spot size resulting from a point source of radiation on the sky can, therefore, be assessed by considering a single pair of instruments — other instrument pairs will contribute structure to the image along different axes, so the width of the central spot can be assessed by simply choosing a representative instrument pair.

In the following, consider the arrangement depicted in Figure 1. A gravitational wave signal $h(t)$ is incident upon two detectors, each of which is a source of noise labeled $n_1(t)$ and $n_2(t)$. If the signal is incident upon the detectors simultaneously, the output of each detector is

$$s_i(t) = n_i(t) + h(t). \tag{2}$$

The correlation integrated over a time T as a function of relative delay Δt is

$$r(\Delta t) = \frac{1}{T}\int_{-\frac{T}{2}}^{\frac{T}{2}} s_1(t+\Delta t/2)s_2(t-\Delta t/2)\,\mathrm{d}t \tag{3}$$

$$= \frac{1}{T}\int_{-\frac{T}{2}}^{\frac{T}{2}} \left[n_1(t+\Delta t/2)+h(t+\Delta t/2)\right]\left[n_2(t-\Delta t/2)+h(t-\Delta t/2)\right]\,\mathrm{d}t. \tag{4}$$

Because there is noise in the detector outputs, r is a random variable. The properties of the noise processes are conveniently described by their power spectral densities, and so it is convenient to use the convolution theorem to express the convolution integral in the frequency domain. That in turn makes it convenient to take the limit $T \to \infty$. However, because the signal is transient, allowing T to grow without bound eventually causes the finite contribution to the integral from the signal to be swamped by the increasing contribution from the noise terms. The problem of assessing the beam pattern for a network that is imaging a transient source such as the gravitational waves emitted from a binary merger is complicated.

In some sense, the short duration of the signal is creating a coupling between itself and the noise: we cannot rely on long-time averages to simplify the arithmetic, and that leaves the results sensitive to the particular realization of the noise that is present at the time of the transient signal.

There are, no doubt, clever ways to analyze the problem. Sonar and radar are obvious examples of the use of aperture synthesis to image transient events, and people must have developed standard techniques to deal with receiver noise. In the interest of expediency, we will simply do the following.

Firstly, momentarily disregarding any concern for our finite-duration signal, we will allow $T \to \infty$, and write the convolution in the frequency domain

$$\tilde{r}(f) \propto \left[\tilde{n}_1(f) + \tilde{h}(f)\right]\left[\tilde{n}_2^*(f) + \tilde{h}^*(f)\right]. \tag{5}$$

Secondly, motivated by the definition of the inner product used to define the "match" in the inspiral search, we will modify our convolution integral by normalizing the frequency-domain detector outputs to the square root of their respective PSDs. For simplicity, let us assume that the detector noise PSDs are identical,

$$\left\langle |\tilde{n}_1|^2 \right\rangle = \left\langle |\tilde{n}_2|^2 \right\rangle = \left\langle |\tilde{n}|^2 \right\rangle. \tag{6}$$

Therefore, the "whitened" Fourier transform of the convolution integral is

$$\hat{r}(f) = \left[\hat{n}_1(f) + \hat{h}(f)\right]\left[\hat{n}_2^*(f) + \hat{h}^*(f)\right] = \hat{n}_1(f)\hat{n}_2^*(f) + \hat{n}_1(f)\hat{h}^*(f) + \hat{h}(f)\hat{n}_2^*(f) + \left|\hat{h}(f)\right|^2. \tag{7}$$

where

$$\hat{X} = \frac{\tilde{X}(f)}{\sqrt{\left\langle |\tilde{n}|^2 \right\rangle}}. \tag{8}$$

Because the noise is a random process, $\hat{r}(f)$ is a random function of f. We can compute its statistical properties from the statistical properties of the noise and the signal. The mean is straightforward; if the noise from the two detectors is not correlated with itself then $\langle \hat{n}_1(f)\hat{n}_2^*(f) \rangle = 0$, and if the noise is not correlated with the signal then $\left\langle \hat{n}_1(f)\hat{h}^*(f) \right\rangle = \left\langle \hat{h}(f)\hat{n}_2^*(f) \right\rangle = 0$, so

$$\langle \hat{r}(f) \rangle = \left|\hat{h}(f)\right|^2. \tag{9}$$

The right-hand side is the convolution of the detector outputs in the absence of noise. In other words, the average or expected "image" is the correct one, the image one would obtain with noise-free instruments.

The variance is

$$\left\langle |\hat{r}(f) - \langle \hat{r}(f) \rangle|^2 \right\rangle = \left\langle \left|\hat{n}_1(f)\hat{n}_2^*(f) + \hat{n}_1(f)\hat{h}^*(f) + \hat{h}(f)\hat{n}_2^*(f)\right|^2 \right\rangle \tag{10}$$

$$= \left\langle |\hat{n}|^2 \right\rangle \left\langle |\hat{n}|^2 \right\rangle + \left\langle |\hat{n}|^2 \right\rangle \left|\hat{h}(f)\right|^2 + \left\langle |\hat{n}|^2 \right\rangle \left|\hat{h}(f)\right|^2 \tag{11}$$

$$= 1 + 2\left|\hat{h}(f)\right|^2. \tag{12}$$

This is an interesting result. The variance tells us how much the amplitude in each frequency bin of the convolution can be expected to fluctuate around it's mean as a result of the random noise in the detectors. This result above tells us that the noise in the image is determined, in part, by the signal: increasing the amplitude of the signal amplifies the noise in the image.

The quantity $\left|\hat{h}(f)\right|^2$ is the Fourier transform of the auto-correlation function of the whitened signal. From (9) and (12), we see that this quantity is entirely responsible for setting the characteristics of the image formed by the detector network of the transient point source. Inverse Fourier transforming this quantity to the time domain yields the average, or expected, image of the point source (as a function of the time delay between the detectors, a quantity easily converted to a direction on the sky).

In what follows, we'll explore the auto-correlation functions of some inspiral waveforms when whitened using the predicted spectra of the Advanced LIGO detectors. We see that this will give a handle on the expected direction sensitivity of a network of detectors in that class.

2.2 Auto-correlation functions

2.2.1 Inspiral Waveform

To begin, we first must look at the merger-waveform for a compact coalescing binary event. The waveform can be defined in the transverse traceless gauge as the linear combination of the two polarizations of the system, $h_+(t)$, and $h_\times(t)$. According to R. Balasubramanian and S. V. Dhurandhar, one of the two polarizations can be chosen for performing analysis due to the contingency that changes in orientation and orbital plane of the binary source only result in changes of amplitude and phase of the signal, not time dependence [3]. Having chosen the $h_+(t)$ component, the waveform is given by

$$h_+(t) = 2.56 \times 10^{-23}\left[\frac{\xi}{3\,\mathrm{s}}\right]^{-1}\left[\frac{r}{100\,\mathrm{Mpc}}\right]^{-1}\left[\frac{f_a}{100\,\mathrm{Hz}}\right]^{-2} a(t)^{-1/4}\cos\left[\frac{16\pi}{5} f_a \xi\left[1 - a(t)^{5/8}\right] + \phi\right] \tag{13}$$

Here t_a is the time of arrival, ϕ is the phase of the merger, f_a is the frequency when coalescing begins, R is the distance to the merger. ξ is the time taken to coalesce and, $a(t)$ is the time-dependent distance between objects (normalized as $a(t_a) = 1$) [3]. The last two parameters are given by

$$\xi = 3.0\,\mathrm{s}\left[\frac{\left[\mu^3 M^2\right]^{1/5}}{M_\odot}\right]^{-5/3}\left[\frac{f_a}{100\,\mathrm{Hz}}\right]^{-8/3} \tag{14}$$

$$a(t) = \left[1 - \frac{t - t_a}{\xi}\right] \tag{15}$$

Where M is the total mass, μ is the reduced mass, and $M_\odot$ is a solar mass [3].

2.2.2 Whitening

We follow our proof by Fourier transforming into the frequency domain, and obtain $\tilde{h}_+(t)$ of our merger-waveform. To convolve our waveforms and produce an image, we must then whiten them with the different Advanced LIGO PSD. These PSD, produced by the seven different science modes, are intended to look for particular waveforms and not just search across a broad-band spectrum like initial LIGO.

Advanced LIGO's increased sensitivity to higher frequencies are scheduled to be implemented first, and are designed to detect neutron star mergers. These are mergers of compact objects that are $1.4M_\odot$ -$1.4M_\odot$. In figure 5, the first three modes are those optimized for neutron star mergers. To be more specific, the first mode does not include signal recycling, i.e. 100% transmission and is most like the initial LIGO configuration (NSNS no SRM). The second mode will have broad-band recycling, which at high power is close to optimization for neutron star mergers (ZERO-DET). The third mode will have full power (125 W) and the signal recycling mirror's (SRM) transmission at 20%, so as to be most detuned to neutron star mergers (NSNS) [4].

The subsequent three modes will be optimized to observe black hole mergers, especially for $30M_\odot$ -$30M_\odot$ inspiral events. The first of which will have no SRM transmission (BHBH no SRM). The second will have the signal recycling cavity (SRC) detuned to 20 ° and SRM transmission of 20% (BHBH 20deg). The third mode will have greater detuning in the SRC and optimization of laser power to create the most favorable mode for observing black hole mergers (BHBH). Finally, the last mode will optimize high frequencies, especially 1000 Hz, by allowing only 1.1% through the SRM and full power (125 W) in the SRC [4]. After obtaining the PSD for each, we look at all seven science modes to determine the sensitivity of each.

Shown in Figures 4 (a) and (b) is the $\tilde{h}_+(t)$ for a $1.4M_\odot$-$1.4M_\odot$ merger and $\hat{h}_+(t)$, the whitened merger-waveform of $\tilde{h}_+(t)$. In comparison Figures 5 (a) and (b) is also shown a $25M_\odot$ - $25M_\odot$ merger and $\hat{h}_+(t)$, the whitened merger-waveform of its $\tilde{h}_+(t)$.

2.2.3 Auto-Correlation Functions

After whitening, we proceed to convolve the waveforms and inverse Fourier transform back to the time domain. This produces an image using the delay between detectors to maximize the resultant function. To aid in the interpretation of the auto-correlation functions, a list of the light travel time which correspond to the maximum time delays between the Hanford, WA observatory (LHO), the Livingston, LA observatory (LLO), and the Pisa, Italy observatory (VIRGO), are listed below [5]. The conversion to θ is shown in Figure 2.2.3.

Table 1: Distances and Light Travel Time Between Observatories

		LHO	LLO	VIRGO
Light Travel Time (s)	LH0	0.0	1.001×10^{-2}	2.729×10^{-2}
	LLO	1.001×10^{-2}	0.0	2.645×10^{-2}
	VIRGO	2.729×10^{-2}	2.645×10^{-2}	0.0
Distance (m)	LHO	0.0	3.002×10^{6}	8.181×10^{6}
	LLO	3.002×10^{6}	0.0	7.929×10^{6}
	VIRGO	8.181×10^{6}	7.929×10^{6}	0.0

Now we present the autocorrelation functions. Shown in Figure 5 is the auto-correlation between $1.4M_\odot$ and $1.4M_\odot$ merger, whitened by the broad-band Advanced LIGO PSD. The full width half maximum (FWHM) is 4 ms. For the LHO-LLO baseline this corresponds to ± 11.49 °,

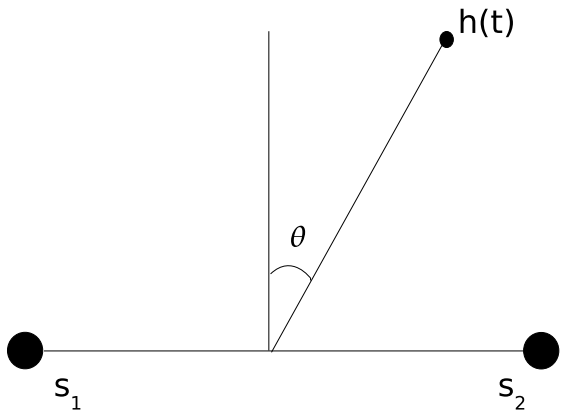

Figure 2: The angle θ is measured from the vertical direction between the two observatories to the source. To convert θ into a time-delay we described Δt by: $\Delta t = \frac{d}{c}\sin(\theta)$, where d is the distance between interferometers, and c is the speed of light

and for the LHO-VIRGO baseline this corresponds to $\pm 4.19\,^{\circ}$, and finally for the LLO-VIRGO baseline this corresponds to $\pm 4.33^{\circ}$. From here we display the auto-correlations for the $1.4M_{\odot}$ and $1.4M_{\odot}$ mergers whitened by the various PSD in Figures 7 (a) and (b). The neutron star modes have a better resolution because they retain higher frequencies after whitening. The higher frequencies result in the sharpening of the peak due to the waveform being forced out of phase more rapidly in convolution compared to those of lower frequencies. This results in a diminished correlation. In Figures 8 (a) and (b), we present the auto-correlations of $25M_{\odot}$ and $25M_{\odot}$ merger whitened by all of the Advanced LIGO PSD and compare them to the $1.4M_{\odot}$ and $1.4M_{\odot}$ mergers. It is observed that the $25M_{\odot}$ and $25M_{\odot}$ merger tend to be broader, again due to the lower frequencies of which they are composed

Finally, we display the auto-correlation functions of $1.4M_{\odot}$- $1.4M_{\odot}$ merger as would be produced using the methodology of the IHOPE coherent step. See Figure 9. The current coherent step uses a match-filter technique to obtain the signal to noise ratio (SNR) as a means of extracting the gravitational wave signal [1]. This is done by convolving the output of the detectors with a template of the merger-waveform to obtain the SNR. In order to adhere to this step, we assumed that the templates are the same as our gravitational wave signal and convolve them first before performing the convolution with the two outputs from each detector. Figure 9 shows the correlation with and without the templates for comparison. The auto-correlation function broadens to a FWHM of 6 ms which corresponds to $\pm 17.39\,^{\circ}$ using the LHO-LLO baseline, $\pm 6.29\,^{\circ}$ using the LHO-VIRGO baseline, and $\pm 6.26\,^{\circ}$ using the LLO-VIRGO baseline. Although the match filter helps to observe a gravitational wave, it does decrease the ability to identify the direction to a source.

For further comparison, M. V. van der Sluys, et. al., preformed a study of parameter-estimation for inspirals using Markov-chain Monte-Carlo methods. During this research they presented their localization ability of initial LIGO. For a binary inspiral with no spin, the accuracy was determined to be $537\,^{\circ 2}$ for two detectors, and $116\,^{\circ 2}$ for 3 detectors. By utilizing the spin of the system, they were able to further constrain the source position to a few tens square degrees [6].

3 Conclusion

Using a representative pair of detectors allows us to approximate the array of observatories as a synthetic aperture imaging system. We are then able to create an "image" of the gravitational wave sources using the auto-correlation method. This image gives us not only the position of the source but also the detection ability from the fringe pattern. By utilizing these auto-correlation functions, one can constrain the limits of directional sensitivity for the Advanced LIGO detectors. Further, it is shown here that the neutron star coalescing binaries, 1.4 $M_{\odot}$- 1.4 $M_{\odot}$ mergers, have a better sensitivity than the black hole coalescing binaries, 25 $M_{\odot}$- 25 $M_{\odot}$ mergers. This is because of the high frequency components that are prevalent in the neutron star waveforms. This is also true for the various PSD tunings, which are optimized for neutron star mergers for the same reason. However, the broadband tuning is more than comparable to any of the specifically detuned modes. Finally, we observed that by modeling the coherent step of IHOPE, may increase the observation

of a compact coalescing binary, but it weakens the sensitivity of the detectors.

4 Acknowledgments

We would like to acknowledge the LIGO Research Program and the funding by the Research Experience for Undergraduates Program of the National Science Foundation.

References

[1] A. Pai, S. Dhurandhar, and S. Bose. Phys. Rev. D **64** 042004 (2001).

[2] A. R. Thompson, J. M. Moran, and G. W. Swenson, *Interferometery and Synthesis in Radio Astronomy*, 2nd ed. (Wiley-VCH, Weinheim, 2001).

[3] R. Balasubramanian and S. V. Dhurandhar. Phys. Rev. D **49** 6080 (1994).

[4] R. Abbott, et. al. http://www.ligo.caltech.edu/docs/T/T070247-01.pdf

[5] source code: LALDetectors

[6] M. V. van der Sluys, et. al. 2008, arXiv:0710.1897v2

5 Figures

Figure 3: Advanced LIGO PSD Tunings

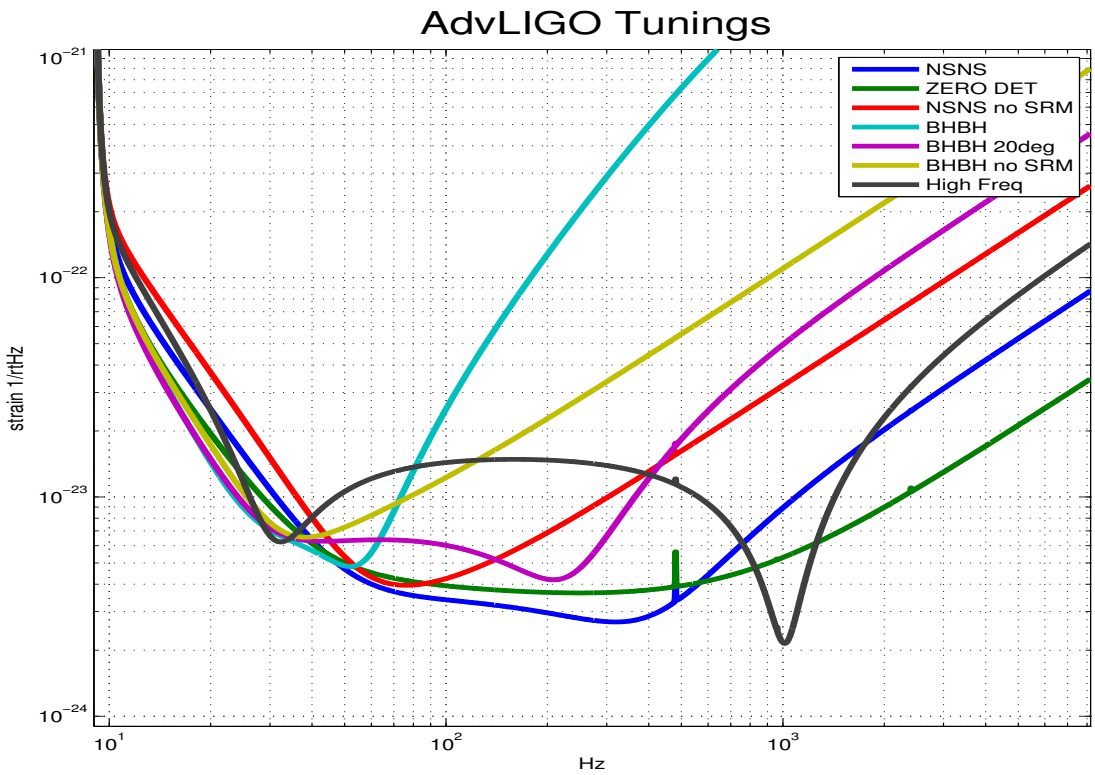

Figure 4: Fourier Spectrums of Neutron Star Merger-Waveforms

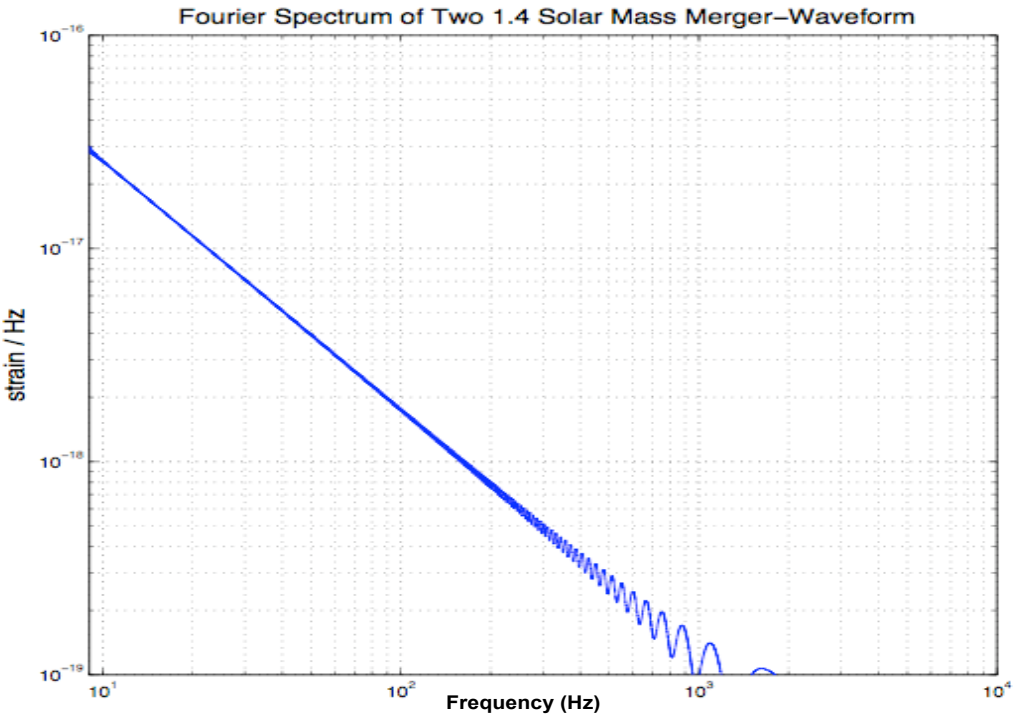

(a) Fourier spectrum of the strain produced by two 1.4 $M_{\odot}$ merger-waveform

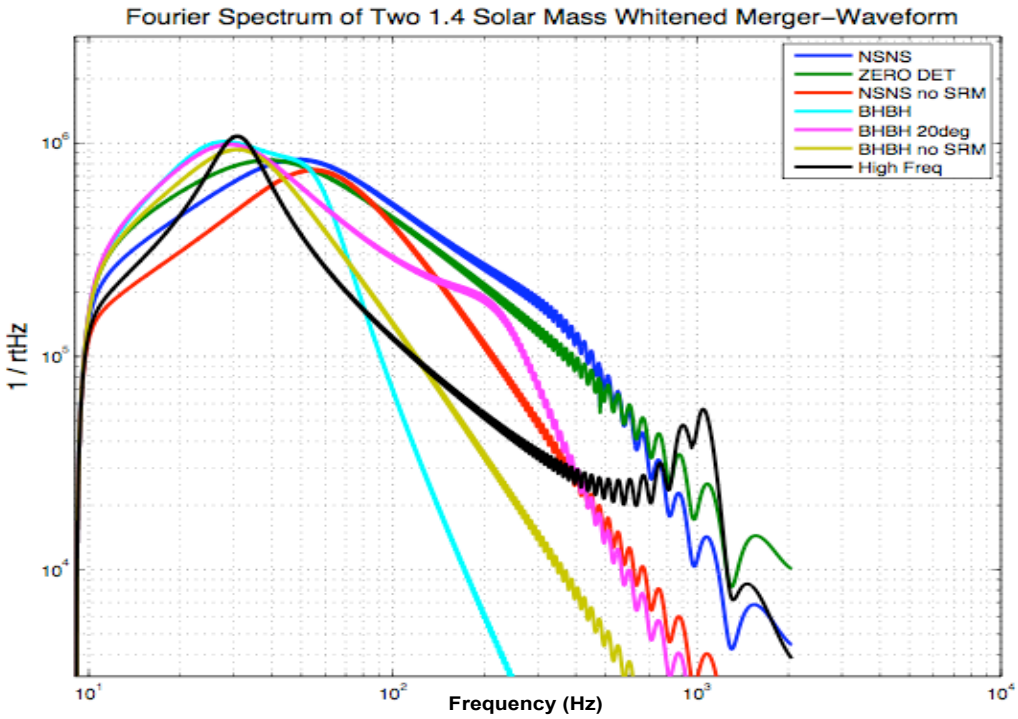

(b) The same Fourier spectrum whitened by the square root of the different PSD tunings of Advanced LIGO.

Figure 5: Fourier Spectrums of Black Hole Merger-Waveforms

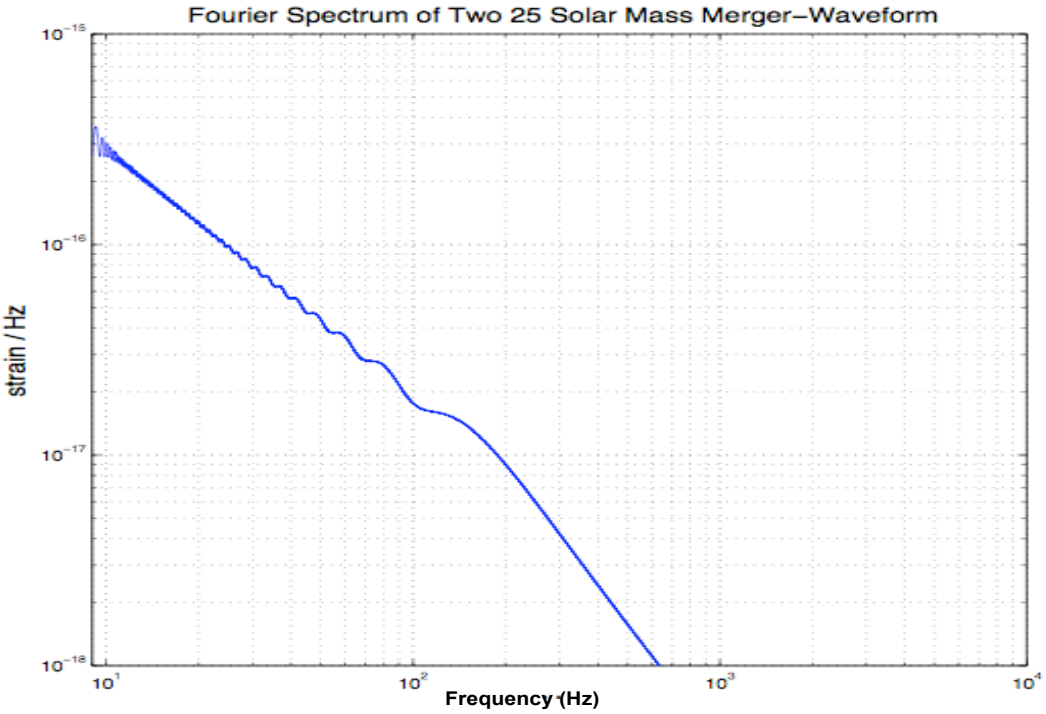

(a) Fourier spectrum of the strain produced by two 25.0 $M_{\odot}$ merger-waveform

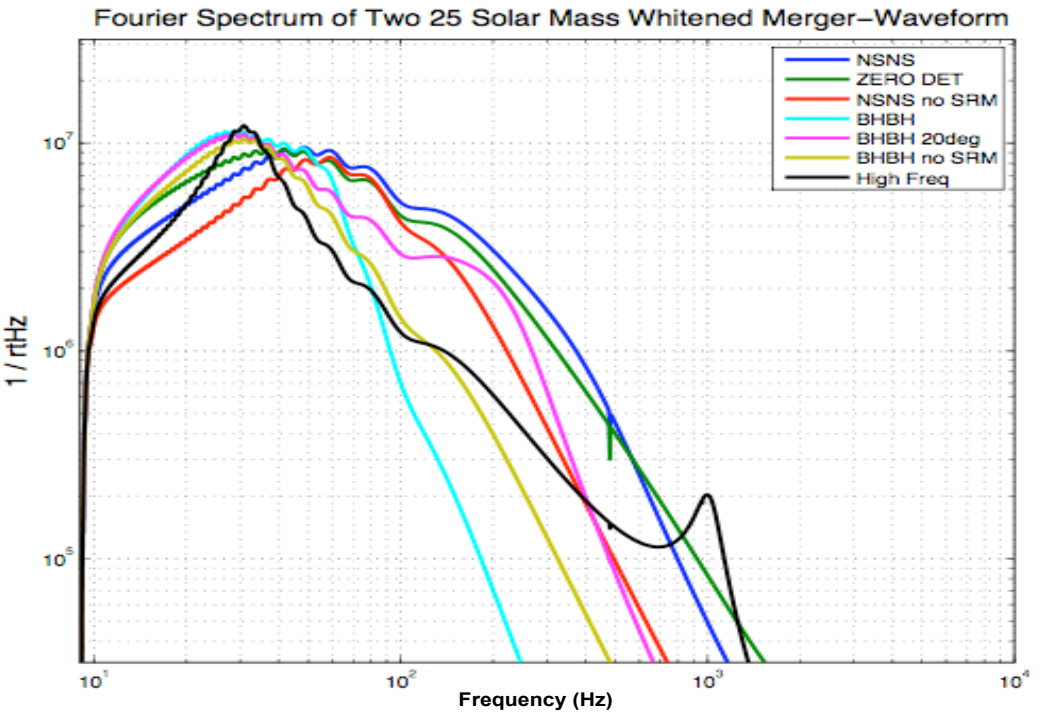

(b) The same Fourier spectrum whitened by the square root of the different PSD tunings of Advanced LIGO.

Figure 6: Auto-Correlation for 1.4 $M_\odot$-1.4 $M_\odot$ Inspiral Merger

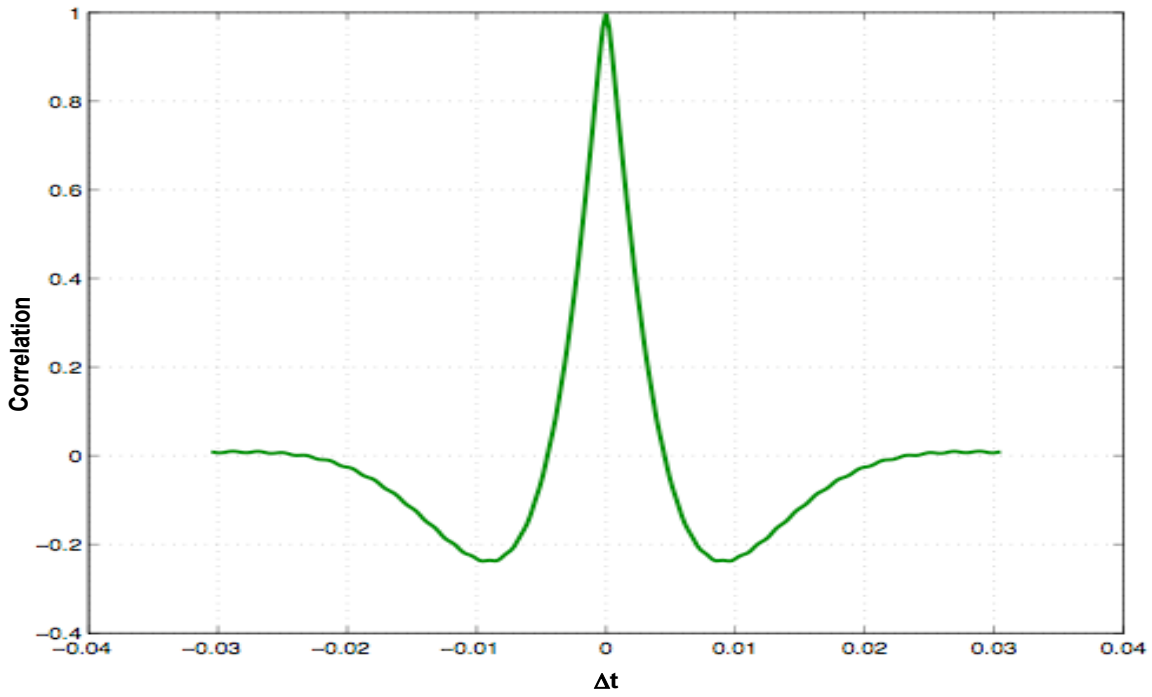

This figure shows the two-point auto-correlation function for two 1.4 $M_\odot$ compact objects' coalescing waveform whitened by the broadband Advanced LIGO PSD. The values are normalized so that 1 is equal to 100% correlation between the two waveforms, and the x-axis is the time-delay.

Figure 7: Auto-Correlation Functions for Neutron Star Mergers

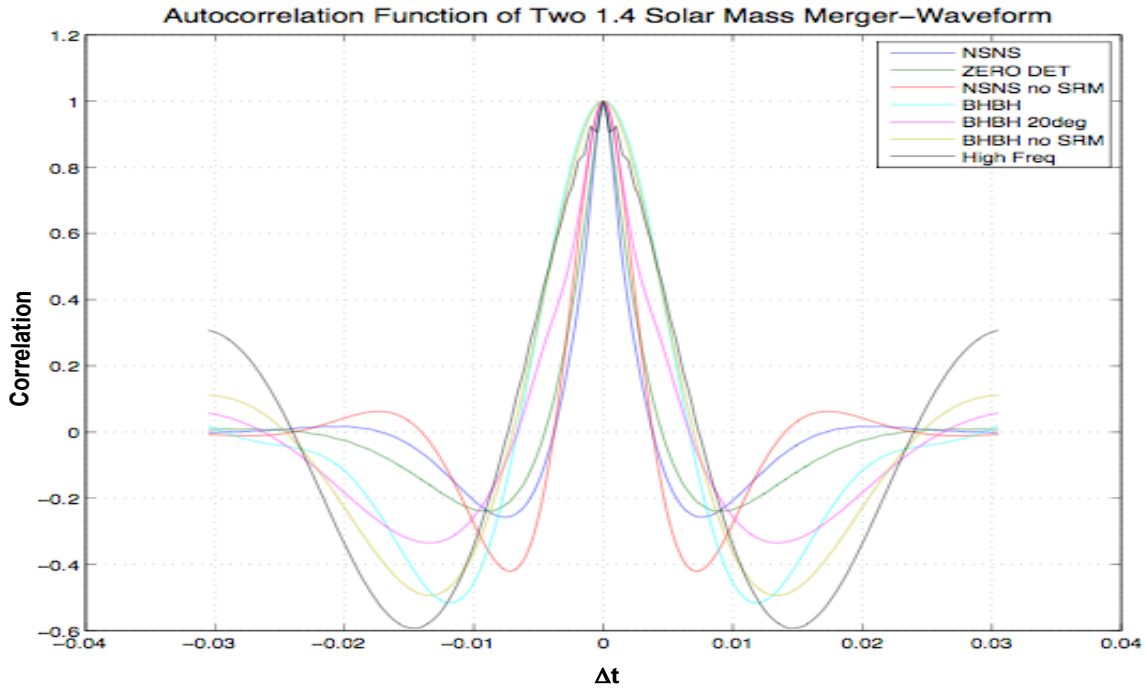

(a) Auto-Correlation Function for 1.4 $M_{\odot}$-1.4 $M_{\odot}$ inspirals with all 7 tunings

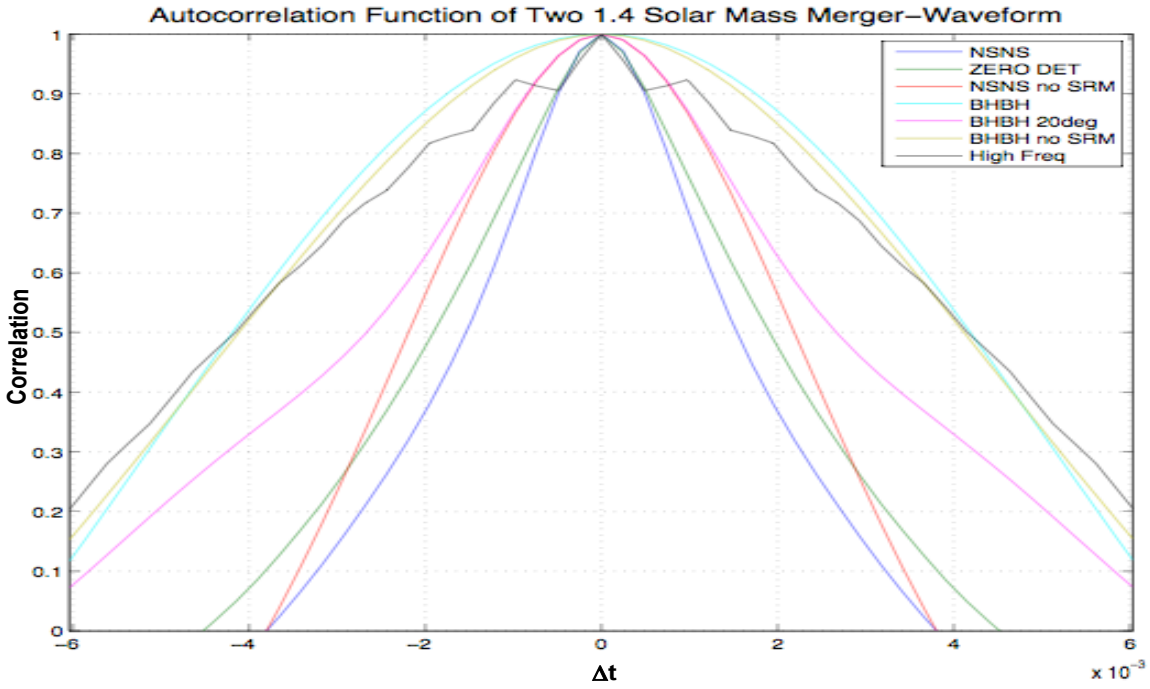

(b) Magnified version of Figure 5 (a)

Figure 8: Auto-Correlation Functions for Both Neutron Star Mergers and Black Hole Mergers

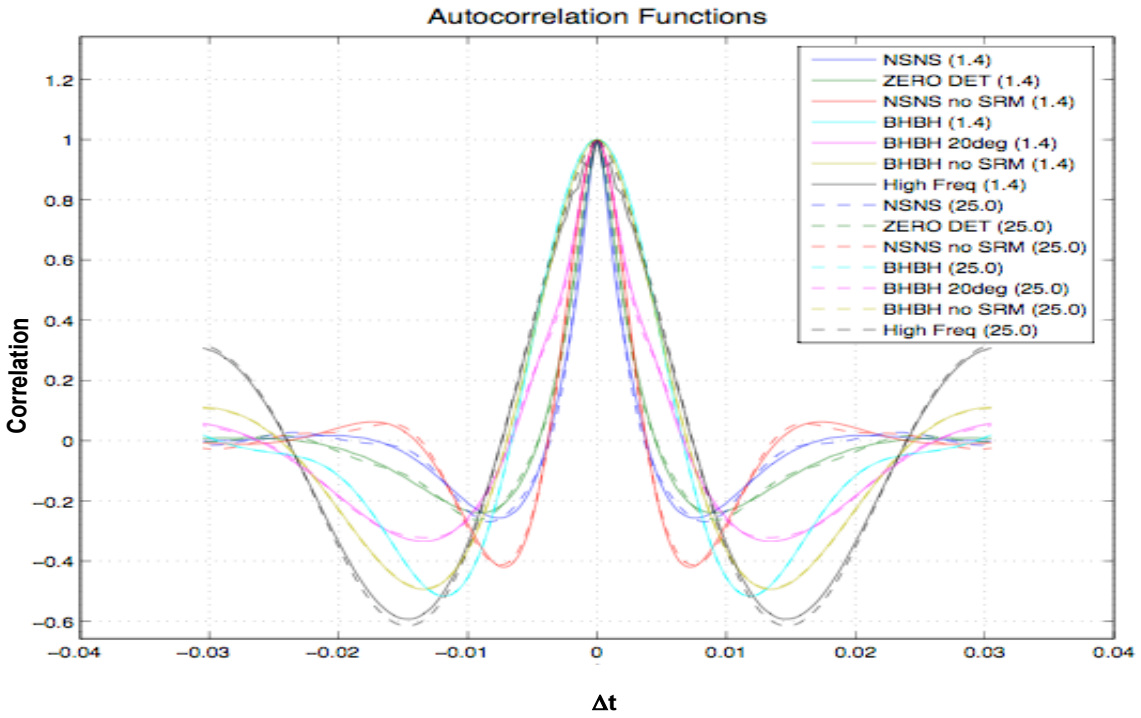

(a) Auto-Correlation Function for 1.4 $M_{\odot}$-1.4 $M_{\odot}$ inspirals and 25.0 $M_{\odot}$-25.0 $M_{\odot}$ inspirals with all 7 tunings

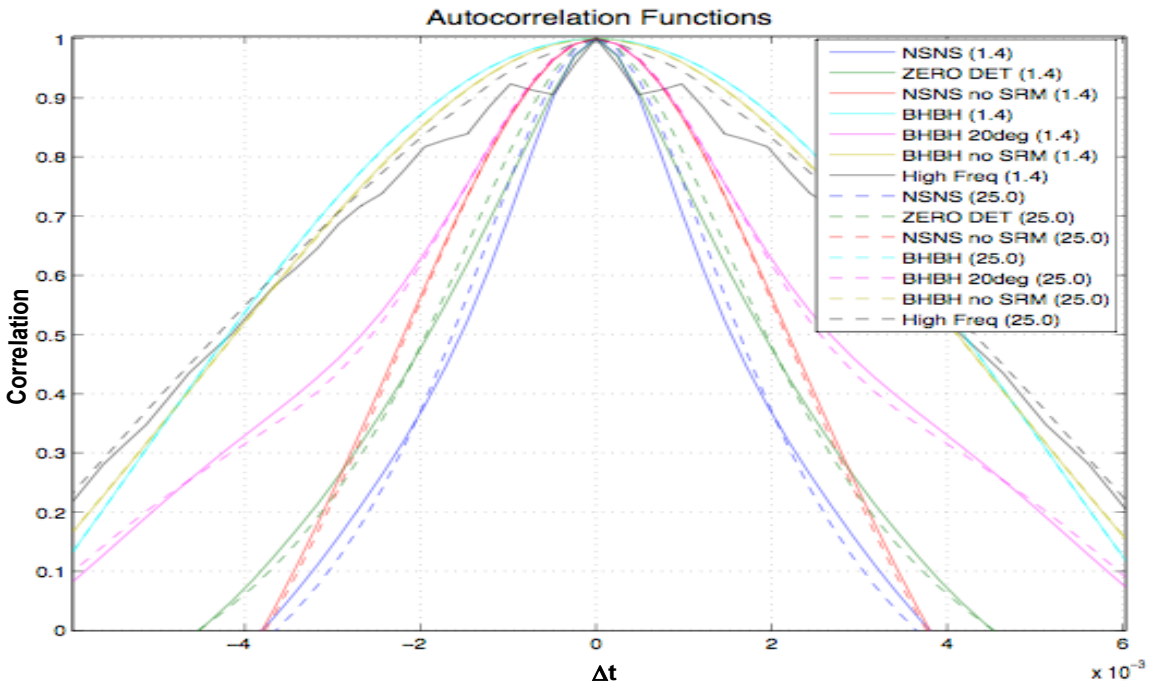

(b) Magnified version of Figure 5(a)

Figure 9: Auto-Correlation for 1.4 $M_{\odot}$-1.4 $M_{\odot}$ Merger-Waveform Convolved with Templates

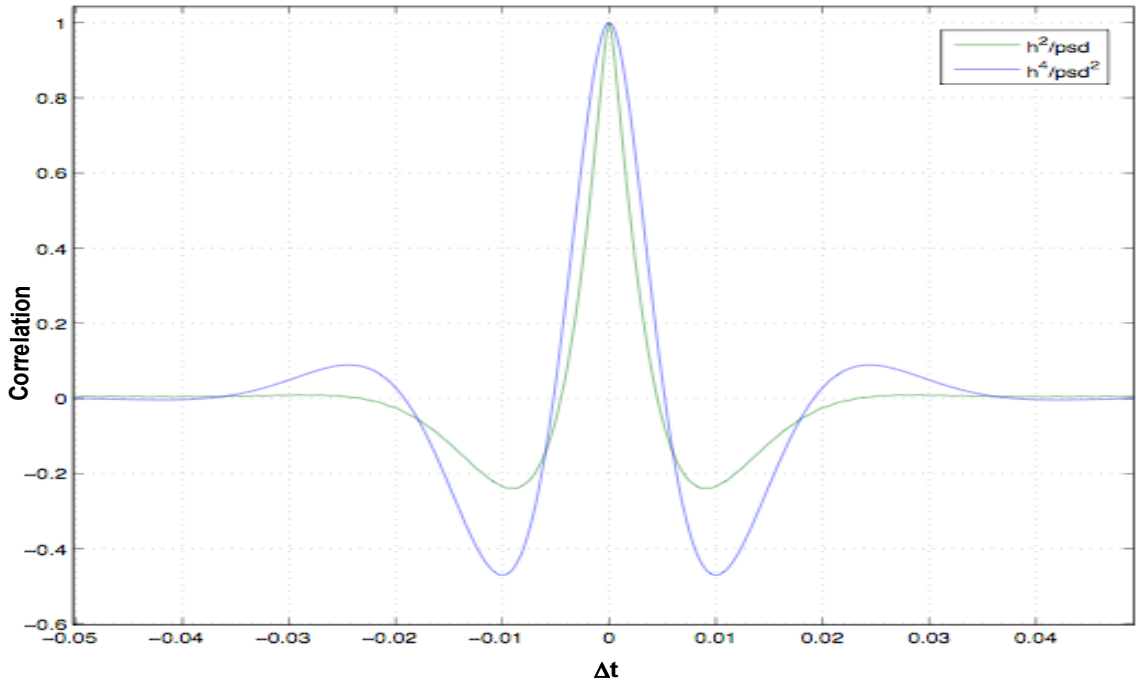

This figure shows the convolution of the output from two detectors that were first match-filtered with templates in blue. It also shows for comparison the convolution of just the outputs in green. Both were whitened by the broad-band Advanced LIGO PSD.